Comparison of algorithms for recognition of cylindrical features in a voxel-based approach for tolerance inspection

Michele Bici[1][0000-0002-7744-2152] and Francesca Campana[1][0000-0002-6833-8505]

[1] DIMA, Sapienza Università di Roma, Via Eudossiana 18, 00184 Rome, Italy
michele.bici@uniroma1.it

Abstract. In injection molding production, automatic inspections are needed to control defects and evaluate the assigned functional tolerances of components and dies. With the "Smart Manufacturing" approach as a point of view, this paper resumes part of a wider research aiming the integration and the automation of a Reverse Engineering inspection process in components and die set-up. The paper compares two fitting approaches for recognition of portions of cylindrical surfaces. Therefore, they are evaluated in the respect of an automatic voxel-based feature recognition of 3D dense cloud of points for tolerance inspection of injection-molded parts. The first approach is a 2D Levenberg Marquardt algorithm coupled with a first guess evaluation made by the Kasa algebraic form. The second one is a 3D fitting based on the RANdom SAmple Consensus algorithm (RANSAC). The evaluation has been made according to the ability of the approaches of working on points associated to the voxel structure that locally divides the cloud to characterize planar and curved surfaces. After the presentation of the overall automatic recognition, the cylindrical surface algorithms are presented and compared trough test cases.

Keywords: Tolerance Inspection, Injection Molding, Random Sample Consensus algorithm.

1   Introduction

In fields like production of electromechanical components through injection molding in multicavity dies, automatic inspections, for die set-up and quality controls of components, are needed to avoid defects and to guarantee the assigned functional tolerances during production. Especially during die set-up, the high number of samples and tolerances to be detected makes the inspection process repetitive and time consuming, to that, many efforts have been spent to increase its automation during acquisition and in data post-processing. In fact, nowadays, automatized procedures are researched and developed not only during the productions or finishing phases [1] but, also, in measurement and control procedures. In previous works [2-5], authors presented procedures oriented to simplify and optimize standard Coordinate Measurement Machine (CMM)

protocols, and to analyse how non-contact measurements may change the data-processing procedures. In the last decade, this kind of issues represented a difficult challenge for researchers in this field [6]. In particular, in this paper, we are going to focus on some new results achieved in a research carried out for integrating the Reverse Engineering (RE) inspection process in the die set-up, so that the final inspection protocol may be automatically filled, performing standard verifications, understanding and analysing dimensional and geometrical deviation of the manufactured surfaces.

The treated research is conducted with a non-contact RE system and original implementations that adopt MATLAB-based algorithms. The hardware system used for the acquisition is composed by a laser scanner (Nikon LC15Dx) mounted on a bridge CMM 3COORD Hera 12.9.7, which, coupled, allow an accuracy of 2,5μm [2-4]. Then, algorithms, developed in MATLAB, are able to perform the data processing and segmentation of the obtained clouds. Finally, measurement algorithms are able to produce data that are useful in PDM. In the electromechanical field, injection molded components are mainly characterized by planar and cylindrical surfaces, with sharp angles, low thicknesses and many small ribs. Therefore, difficulties arise not from the characteristics of surfaces, but from the necessity of procedure automation on hundreds of samples. In [2], an original voxel-based implementation has been proposed to distinguish planar surfaces in electromechanical parts. Non-planar regions have been then investigated in [3, 4], so that, cylindrical surfaces may be recognized and measured according to a 2D fitting algorithm, developed starting from Kasa formulation. This paper compares this algorithm with another one, called Maximum Likelihood Estimate SAmple Consensus algorithm (MLESAC), and based on RANdom Sample Consensus algorithm (RANSAC). After a brief outline of the previous developments in Section 2, Section 3 presents the new approach and, then, in Section 4, some case studies, used to develop and test the procedure, are presented and discussed. Finally, in Section 5, major conclusions are highlighted.

2 Previous developments

RE encompasses several tools and methods suitable to make digital models of real parts. As reported in [7, 8], generally, they can be divided in a sequence of four steps: (1) Data Acquisition; (2) Data Processing; (3) Segmentation and Surface (or feature) Fitting; (4) CAD Model Creation. The reported research is focused on the development and test of algorithms of data processing, feature segmentation and recognition (phases 2 and 3). The general workflow and phases of the developed procedure are reported in Figure 1, [4] and explained in the following.

2.1 Voxel structure

The adoption of voxel-based approach was defined considering the requirement of decreasing the post-processing duration. Although gradient analysis is one of the most adopted solutions [9, 10], it is clear that the number of points, their density and distribution influence the analysis accuracy. This problem is partially solved by filtering

[11], but, in case of tolerance analysis and quality inspection, it may lead to a loss of data. Moreover, surface reconstruction of filtered acquisition may not represent a good solution, even if adaptive filtered, due to high computational time. For these reasons, supported also by [10], we decided to work with a voxel-based approach that localizes volumes according to a semantic significance, which in our case is a specific feature of the shape (planar/curved, planar/cylindrical). This kind of segmentation is related to a problem of feature recognition [12]. Doing so, we can analyze the surface recognition problem according to a scale larger than the tessellated mesh, without applying preliminary filters, or classical segmentation through curvature [13]. One of the advantages of the approach consists in avoiding mesh triangulation and point evaluation of local curvatures that are substituted with local surface reconstruction of the points inside voxels. Another peculiar point that has to be noticed is the fact that the usage of voxel segmentation, in this way, make the amount of segmentation elements not directly dependent from the point density and distribution.
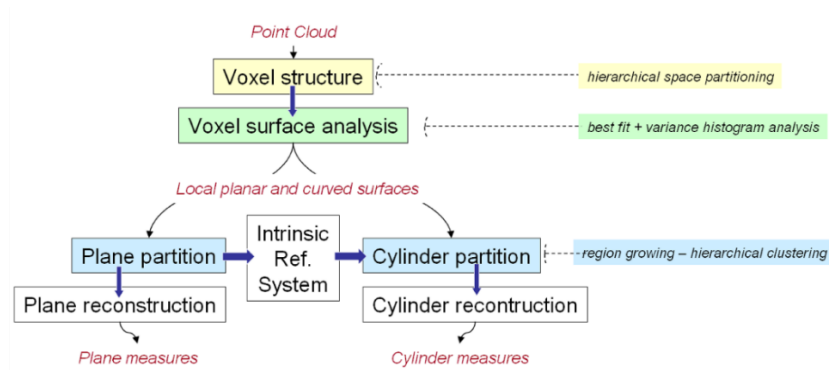
Fig. 1. The developed procedure for data processing, segmentation and surface fitting, [4].

The voxel-based approach is based on a grid method similar to an octree grid derived from hierarchical space partitioning [14]. In our case, a 3D voxel structure is superimposed on the acquired cloud of points. It is defined through an iterative procedure that starts from a single parallelepiped. It encompasses acquired cloud completely, then, along each direction (x, y and z), it is recursively split into smaller volumes, generating a voxel structure, until no more points are included into an element or if the assigned limit of a voxel size is reached. The final structure made with the smallest size voxel represents the voxel structure of the partition. In [2, 3], implementation details related to the voxel structure definition are described and discussed. From this part of the research, it resulted how the voxel ratio and dimensions influence the following results. Due to this, some procedures and tests to optimize the voxel lengths and ratio have been developed for each kind of component (prismatic, axisymmetrical and boxed-shape components).

4

2.2   Voxel surface analysis

Once the voxel discretization is performed, local surface recognition starts through the computation of geometric descriptors. Local surface recognition is carried out through best-fitting algorithms. Electromechanical parts made by injection molding are predominantly feature-based shapes, thus plane inspection is the starting part of our segmentation. For this reason, voxels with planar surfaces are firstly detected, through threshold analysis of the fitting parameters [10, 15]. The threshold works on the variance of the point distances from the local plane fit in the voxel. Thanks to the accuracy of the acquisition, planar surfaces populate always the first bin of the variance distribution on the voxels. The bin major value can be assumed as a threshold to exclude all V_{ijk}, which are filled with points that lay on curved surfaces. Optimal values for thresholds can be found with an iterative procedure, already developed, and explained in [4].

Local surface recognition is approached by fitting. In the first phase, for each "true" state voxel, a local plane is fit by least square minimization, through Single Value Decomposition, obtaining the geometrical descriptors parameters of each local plane. Voxel that do not present geometrical descriptors parameters inside the threshold are associated to "curved" local surfaces. They can be free-form or cylindrical or boundary voxels. In any case, finding their geometrical descriptors, which means recognizing a specific type of surface, means assuming a specific equation to be fit. In Section 3, the problem of the local fitting of cylindrical surfaces is provided.

2.3   Region growing

Following the procedure reported in Figure 1, according to the threshold analyses, the voxel structure is partitioned in planar, cylindrical and other curved voxels. From this distinction, the global recognition of the component planes or cylindrical surfaces may derive by means of a region growing algorithm [4, 16]. This kind of algorithm is able to aggregate together, according to an imposed threshold, contiguous voxels that have similar geometric descriptors (normal direction and distance from the origin, in the case of planes; axis and radius, in case of cylinders). Region growing algorithms define clusters starting from "seeds" able to describe a feature. In planar voxels case, the unit vectors associated to the normal of the best-fit planes inside the voxels, $(n_x\ n_y\ n_z)_{ijk}$, are verified to a specific unit direction, (a b c), by means of a threshold condition derived from the so-called L_2 orientation norm [2, 10] and to an adjacency matrix. This procedure, based on Single Value Decomposition, explained in [2], consent to perform the plane clustering according to every significant direction of the acquired components that are found in S.

Analogously, in cylindrical voxel, after the local fitting explained in the following section, regardless of the fitting procedure chosen, the clusterization is made according to seeds found from other suitable descriptors, as radius, considering that the aggregation by means of the axes is taken into account by the voxel connection and proximity. This conduct to obtain a cylindrical clustering according every significant radius of the component. Result of clusterization is the global surface recognition. By that, all the

found global features, planar or cylindrical, can be submitted to the measurement procedure, explained in [5], able to perform tolerance control and to insert the result in a PDM file regarding the component, arriving to evaluations of dies and suppliers.

3 Fitting of cylindrical surfaces inside curved voxels

In this section, the problem of finding cylindrical surfaces is faced. According to Fig. 2 it requires a proper local surface analysis inside the voxels associated to curved surfaces, then region growing based on eq. 2 must be run.

3.1 LM(Kasa) approach

As first approach, local cylindrical surfaces have been recognized through a fitting strategy that is related to a common practice in CMM inspection: circle fitting of sections [4]. Circle fitting can be approached by geometric or algebraic fits. In the first case, the unknown parameters (position of the centre, C, and radius, R) are found through an iterative regression process, as, for example Levenberg-Marquardt (LM). Algebraic approaches like Taubin or Kasa [17, 18]. Kasa is the fastest method that works with good results in case of complete circles but it loses accuracy in case of points along arcs with small diameters. Regression approaches, like LM, are strictly related to the adopted first guess, moreover local minimum cannot be excluded. As reported in [4], our firstly developed application, LM(Kasa), couples together Kasa and LM, using Kasa to give a rough estimation of the curved voxel surface that is used as first guess of LM. It has been demonstrated that LM(Kasa) is, at least, performant as Taubin or even more, in some different conditions (high or scattering level, small and large arc lengths, small or high values of R).

Major problem related to LM(Kasa) approach is the necessity of finding proper projection directions, to find circular sections. It has to be associated with the concept of Intrinsic Reference System (IRS), treated in the following, and to the hypothesis of having pins and holes with axes along this reference system.

For satisfying this hypothesis, from the voxel structure over-imposed on the component, an IRS may be found, looking for the plane directions associated to the most populated sets of voxels. In our case, in fact, it resulted that it may be assumed as a consistent reasoning since these injection molded components are characterized by functional features on orthogonal planes or cylinders whose axes are parallel to three principal directions of the component. Thus, the most populated set of voxels are the ones that contain planar surfaces oriented along principal directions of the component. By this, The IRS computation derives, assigning as first reference axis the planar direction of the most populated set of voxels. Then the other two axes are found between the two subsequent more populated sets, mutually orthogonal, as tested in [3].

6

3.2   RANSAC approach

To release cylinder fitting from IRS, point projection may be avoided. Thus, a second fitting strategy has been investigated. It works with a RANSAC-based algorithm, offering a more generalized approach to all the kind of surfaces, also planes [19, 20]. It is an iterative algorithm, able to fit the model parameters in case of data with noise. It starts with a preliminary evaluation of the model on a minimal data set, taken randomly from the point cloud. After this, the remaining points are checked concerning their significance with the adopted thresholds (statistical confidence of the parameters, inlier maximum distance from the evaluated surface). If they are not significant, they are evaluated as outliers. The evolution is iterative until the confidence is reached and, obviously, a proper model must be selected. In our case, to avoid the use of the IRS, the first application of RANSAC was made to fit cylinders through the points inside the curved voxels. In particular, we adopted the MLESAC algorithm, found in Matlab 2017. It starts from a sample of 6 points necessary to preliminary estimate the cylinder axis. Required thresholds are the maximum distance from the surface, to be an inlier point and the confidence (default 99%). Obviously, sometimes the algorithm may fail to evaluate an axis direction, thus a first guess must be provide. It means that, in a certain way, in some critical cases, MLESAC algorithms cannot work without a first guess information, connected to the axes. In general, it resulted that they are IRS-dependent, in some cases, as LM(Kasa) procedure is. In addition, a preliminary set-up of the proper thresholds for the maximum distance inlier-surface and confidence must be done.

Sensitivity analysis for RANSAC parameters. The first goal of the research activity is the evaluation of the sensitivity of the algorithm in the respect of the threshold analysis. We investigated if local fitting inside curved voxels is robust enough to provide a threshold for the next region growing. The sensitivity analysis has been carried out on the maximum distance, from the evaluated surface, used to define inliers and outliers. It has been made and compared with a least squares error fit, made in Catia V5.Two sets of points, one representing a whole cylindrical surface, the other only a portion, have been used (Figure 2). Their parametes are resumed in Table 1. The following Figures 3(a) and 3(b) resume the performed sensitivity analyses. Maximum distance (the abscissa) is correlated to the entity of "noise" present. A reduction of this value makes more stringent the evaluation of the "inlier condition", assignable to data points.
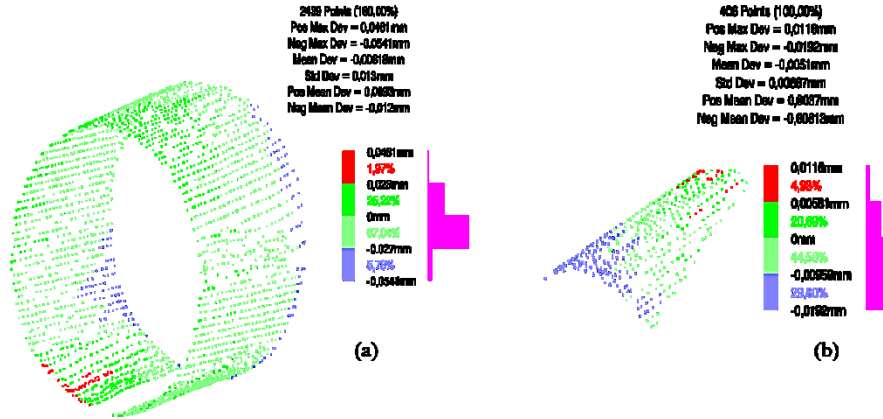
Fig. 2. Distance analysis from the cylinder fit made by CatiaV5R12: (a) Point cloud #1; (b) Point cloud #2.

Table 1. Fitting parameters found by CatiaV5R12.

	Point Cloud #1	Point Cloud #2
No. of points	2439	406
Estimated radius (mm)	0,9728	1.0103
Axis direction (mm)	[0.999, -0.007, -0.002]	[0.999, -0.360, -0.0165]
Mean error (mm)	0,0094	0.0055
Standard dev. error (mm)	0,0087	0.0033

To understand this effect, we have imposed a range for the distance from 0.5×10^{-3} mm to 0.06 mm with steps of 0.25×10^{-3} mm. These values, as said are reported as abscissa of the figures. The plot in the upper part of both show the fitting mean error in respect to MaxDistance. Smaller values of MaxDistance decrease the mean error, and obviously the number of inlier points, as reported in the graphs at the bottom of Figure 3. Plots in the middle represent the trend of Radii of cylinders, varying the MaxDistance. For Figure 3(a), a stable trend for Radius can be seen at about 0.97 mm, with a high scattering when MaxDistance increases. This is not suitable and consistent from a tolerance inspection point of view. It confirmed the necessity of a rule to define the Max Distance For this reason, through the comparison with Catia fittings, we investigate the Max Distance ranges nearby the maximum deviations (respectively 54.1×10^{-3} mm and 19.2×10^{-3} mm) of the distance analyses (Figure 2). Doing so we are assuming that small probability of noisy data may occur and all the points can be inserted in the MLESAC computation, as in a standard fit. For first cloud, in a range of MaxDistance equal to 0.04÷0.06mm (in red in Figures 3(a) and 3(b)), we found a fitting error of 0.017±0.004mm and a Radius of 0.9686±0.0157mm. Analogously, for the second set, in a range of 0.015÷0.025mm, we found a fitting error of 0.0053±0.0017mm and a Radius of 1.0117±0.0644mm
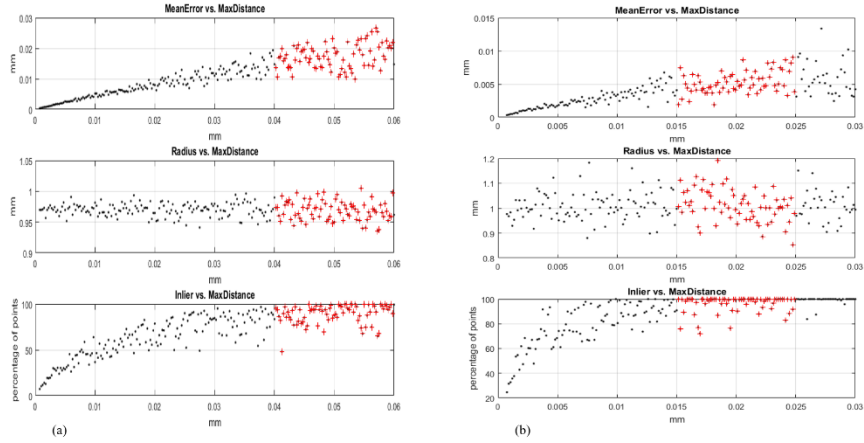
Fig. 3. Sensitivity Analysis according to the input parameter related to the maximum distance of the inliers from the evaluated surface (MaxDistance). Upper plot: Mean Error of the fit; Middle plot: Radius of the fitting; Lower plot: percentage of inliers in the respect of the total number of points: on the left Point Cloud #1, on the right Point Cloud #2.

4 Set-up and evaluation of the algorithms through case studies

Two different case-studies are reported: a flange and a latching lever. Both components have been used for set-up of the algorithms and their tests.

### 4.1 Flange for Aeronautical applications

Fig. 4. Flange for aeronautical applications.

The flange is not an injection molded part, but it has been selected, as testing case study, and already used in [3], to stress the algorithms with large shapes and curvatures, and details in a wide range of lengths. It is a component of a Boeing product, obtained through β-forging starting from Ti_6Al_4V Titanium alloy powders. Characteristic lengths are 208x208x30 mm, and after multiple view alignment, a point cloud of about 480000 has been obtained. Due to the fact that our focus is on cylindrical fitting, other parameters and parts of the entire procedure will be not treated here (as voxels subdivision

and threshold analysis) and considered as optimized for LM(Kasa) (it is used a voxel structure of 64x64x16). As said, LM(Kasa) asks for a preliminary knowledge of the axes directions, MLESAC does not, with some exceptions. For LM(Kasa), a component IRS is defined through a specific elaboration of the most populated planar clusters that are derived from the voxel structure. In the flange case, the calculated IRS has the x-axis coincident with the longitudinal axis of the component. Therefore, LM(Kasa) assumes that axes directions of the founded cylinders are oriented as the x-axis of the IRS. This assumption is consistent with datum references. A good resolution of the proposed method has been confirmed also by the map of voxel osculating radii of the cylindrical features. The surface reconstruction of the cylinders has revealed 0.02mm of tolerance from the nominal value and a good predictable ability of this kind of algorithm [3].

Regarding MLESAC algorithm, for the flange and the imposed voxel structure (64x64x16), it has been found that, in over the 30% of the voxels recognized as curved, the algorithm failed the surface fitting. This because of a low amount of points within each of these voxels (less than 6 points). This convinced us to use a less accurate voxel structure (32x32x16). The obtained result, reported in Figure 5, demonstrated a not accurate fitting and recognition. Table 2 demonstrates this hypothesis according to a reduction of the number of voxels, thus, to an increase of the average number of points per voxel.
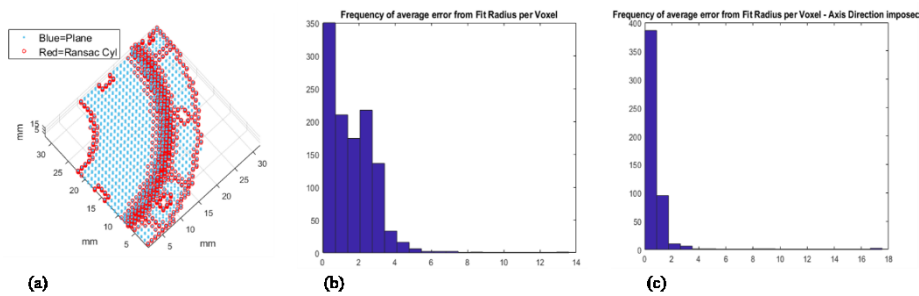
Fig. 5. (a) Final voxel partition in Cylindrical and Planar local surfaces; (b) Frequency distribution of the occurrence of the mean of the distance errors from the fit radius without axis imposition; (c) Frequency distribution of the occurrence of the mean of the distance errors from the fit radius with axis imposition.

More in detail, it shows a high scattering in terms of mean of the distance error among points in the cylindrical voxels and fit radius, the population of bins higher than first or second can be interpreted in this way. This represent the high difficulty of fitting cylinders with large curvature. Figure 5(c) shows the situation of the mean error distribution after the axis imposition. It seems to be improved for what concerns the possibility of finding a threshold able to divide inliers from outliers, performing a huge improvement for large curvature cylinders, but it resulted to have a higher number of failed curved voxels to be fitted as cylinders (up to the 60%). This makes the results obtained by MLESAC, in both forms, less accurate than the LM(Kasa) ones.

Table 2. Percentage of curved voxels that fail to find MLESAC solution – Maximum distance set to 0.1 mm, confidence=99%.

Resolution	V_{ijk} length (mm)	% of curved V_{ijk} that fail MLESAC
16x16x16	6.5x.6x1.9	1.50%
32x32x16	3.2x3.2x1.9	8.40%
64x64x16	1.6*16*1.8	35.80%

4.2 Latching Lever

In order to test the two strategies, another case study has been analyzed. It is an injection molded Latching Lever, used in assemblies of electromechanical switches of electric panels, made in PPS. Characteristic lengths are about 20x10x4 mm, more than one sample has been acquired obtaining, after multiple views alignment, point clouds of over 60000 points. We used this case study to evaluate performances of LM(Kasa) in comparison to the results obtainable through MLESAC, adopting, as imposed axis for the fitting, the same direction used in LM(Kasa). Using a 32x32x32 voxel structure, the local surface recognition of planar and curved featured is represented in the right side of Figure 6.
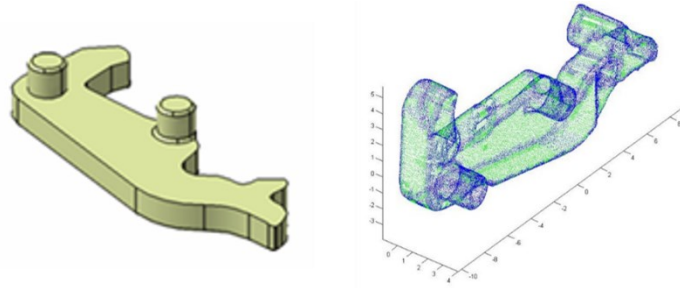

Fig. 6. Nominal CAD model of the Latching Lever (on the left); local surface recognition of planar feature, in green, and curved ones, in blue (on the right).
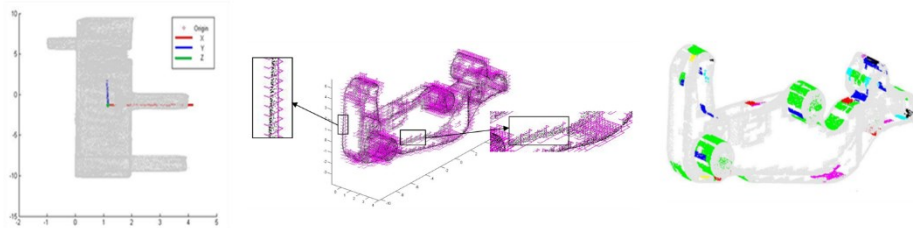

Fig. 7. The calculated IRS for the lever (on the left); curved voxel partition (in the middle); cylindrical feature recognition through LM(Kasa) (on the right).

From the planar voxel clusterization, the IRS has been found. As already mentioned, the cylindrical features appear, also in this case, to have axis directed according to one

of the principal direction, found through voxel population. In fact, in the lever, the x-axis resulted to be the one coincident with the directions of the two cylinders and the rounds present (on the left of Figure 7). The cloud has been partitioned according to the found IRS, and the curved voxel are represented in the middle of Figure 7. Then, cylindrical features, through LM(Kasa), have been obtained, as showed on the right of Figure 7. To give an evaluation of this approach, cylinders A, B and C of Figure 8 have been compared with interactive post-processing made by Catia. In this case, Cylinder A has an effective value of R=0.974 mm, we also obtained R=0.972 mm (for Cylinder B) and R=0.999 mm (for Cylinder C). Standard deviation of the fittings are always less than 0.012 mm. Through the proposed algorithm, the radii of each feature are: 0.974 mm for cylinder A and B, 1.036 mm for cylinder C with a standard deviation less than 0.006 mm. Using MLESAC with imposed axis (1, 0, 0) as input parameter, similar results have been obtained, but improved in the detection of the common radii along the voxels on the width of the free form part (Figure 9).
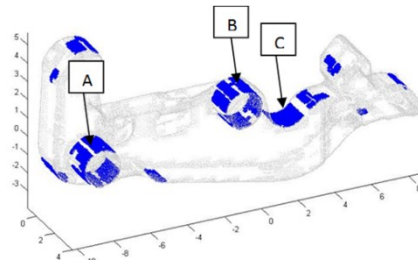
Fig. 8. Selected cylinders with R = 1mm.
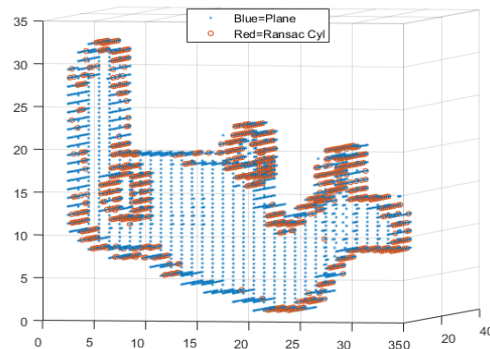
Fig. 9. MLESAC with imposed axis (1,0,0) applied on Latching Lever.

4.3 Discussion

For what concerns the case study of the flange, it can be said that LM(Kasa) showed good results despite the fact that asks for preliminary knowledge of the cylinder axis

directions, taken out by the IRS calculation. MLESAC may avoid this request, not in totality of cases, but more problems arise to find a proper threshold for affirming that the voxel is cylindrical with any doubt. It is due to problems about finding large curvature cylinders through points on a small arc length, when no axis direction is given as first guess. This makes the fit model highly scattered also among contiguous curved voxels, ruining the region growing – hierarchical clustering of large radius areas. Imposing a first-guess direction, many curved voxels are not fit (60%), but radius evaluation highly improves. Concerning cylindrical fitting for the flange, MLESAC cannot overcome the problems of LM(Kasa) that results more reliable for large curvature cylinders through points distributed on a small arc length. On the contrary, in features with lower values of radii, as for latching lever, the two strategies can drive to similar results. It has to be noticed that also in this case, in order to perform a significant recognition, MLESAC needed the first guess, with the imposition of the cylinder axis direction, failing again to what we had thought could be a huge advantage of this method, proved instead to be not so disruptive, as depicted also in literature, in respect to that previously developed.

5   Conclusions

In this work, two kinds of algorithms for cylindrical feature recognition have been compared. One, LM(Kasa), already developed by the authors in the past, had already proved to be reliable and moderately accurate, presenting the disadvantage of being a 2D processing of points to be fit, so requiring the axis direction of the cylinder to be recognized. Due to this disadvantage, after a literature research, authors developed another procedure, based on RANSAC algorithms. The main advantages of this procedure, as depicted in the literature, were mainly connected to the possibility of avoiding a first-guess (6 points, so, a direction), thus, recognizing cylinders without the dependence from the definition of an IRS (Intrinsic Reference System).The comparison has been made through two different case studies: a flange for aeronautical application and a latching lever for electromechanical of electric panels. Due to the differences between the case studies, it has emerged that for what concerns cylinders with high radii, LM(KASA) performs better than MLESAC. In addition, this second approach revealed its needing of a first-guess direction exactly as LM(Kasa), but without arriving to the same level of accurate recognition. For what concerns cylinders with smaller radii, as the features present in the lever, the two developed algorithms resulted to be quite similar, depending both by the imposition of the axis of the cylinder to be recognized and performing results with the same level of accuracy. Further researches and tests are needed in order to obtain a more accurate evaluation of these algorithms, but this comparison showed that the already developed algorithm, LM(Kasa), remains currently the best and more robust choice for performing cylindrical feature recognition oriented to tolerance inspection and quality controls.

Acknowledgements

References

1. Hähnel, S., Pini, F., Leali, F., Dambon, O., Bergs, T., Bletek, T.: Reconfigurable Robotic Solution for Effective Finishing of Complex Surfaces. 2018 IEEE 23rd International Conference on Emerging Technologies and Factory Automation (ETFA), Turin, Italy, 1285-1290 (2018).
2. Bici, M., Campana, F., Petriaggi, S., Tito, L.: Study of a Point Cloud Segmentation with Part Type Recognition for Tolerance Inspection of Plastic Components via Reverse Engineering. Computer-Aided Design and Application, 11(6), 640-648 (2014).
3. Bici, M., Campana, F., Trifirò, A., Testani, C.: Development of automatic tolerance inspection through Reverse Engineering. 2014 IEEE Metrology for Aerospace (MetroAeroSpace), Benevento, Italy, 107-112, (2014).
4. Bici, M., Campana, F., Trifirò, A.: Automatic post-processing for tolerance inspection of digitized parts made by injection moulding. Computer-Aided Design and Applications, 13(6), 835-844 (2016).
5. Bici, M., Broggiato, G. B., Campana, F., Dughiero, A.: Computer Aided Inspection Procedures to Support Smart Manufacturing of Injection Moulded Components. Procedia Manufacturing, 11, 1184-1192 (2017).
6. Germani, M., Mandorli, F., Mengoni, M., Raffaeli, R.: CAD-based environment to bridge the gap between product design and tolerance control. Precision Engineering, 34(1), 7-15 (2010).
7. Varady, T., Martin, R. R., Cox, J.: Reverse engineering of geometric models - an introduction. Computer Aided Design, 29(4), 255-268 (1997).
8. Bradley, C., Currie, B.: Advances in the Field of Reverse Engineering. Computer-Aided Design and Applications, 2(5), 697-706 (2005).
9. Attene, M., Falcidieno, B., Spagnuolo, M.: Hierarchical mesh segmentation based on fitting primitives. The Visual Computer, 22(3), 181–193 (2006).
10. Shamir, A.: A survey on Mesh Segmentation Techniques. Computer Graphics Forum, 27(6), 1539–1556 (2008).
11. Ali, F., Chowdary, B. V., Imbert, C. A.: Part design and evaluation through reverse engineering approach. International Journal of Agile Manufacturing, 11(1), 73-82 (2009).
12. Di Stefano, P., Bianconi, F., Di Angelo, L: An approach for feature semantics recognition in geometric models. Computer-Aided Design, 36(10), 993-1009 (2004).
13. Attene, M., et al: Mesh Segmentation - A Comparative Study. IEEE Computer Society, Washington, DC, USA (2006).
14. Keller, P., Hering-Bertram, M., Hagen, H.: Reverse engineering with subdivision surfaces. Computing, 79(2-4), 119-129 (2007).
15. Courtial, A., Vezzetti, E.: New 3d segmentation approach for reverse engineering selective sampling acquisition. The International Journal of Advanced Manufacturing Technology, 35(9), 900-907 (2008).

14

16. Lee, Y., Park, S., Jun, Y., Choi, W. C.: A robust approach to edge detection of scanned point data. International Journal of Advanced Manufacturing Technology, 23, 263-271 (2003).
17. Taubin, G.: Estimation of planar curves, surfaces, and nonplanar space curves defined by implicit equations with applications to edge and range image segmentation. IEEE Transactions on Pattern Analysis and Machine Intelligence, 13(11), 1115-1138 (1991).
18. Kasa, I.: A circle fitting procedure and its error analysis. IEEE Transactions on Instrumentation and Measurement, IM-25(1), 8-14 (1976).
19. Schnabel, R., Wahl, R., Klein, R.: Efficient RANSAC for point-cloud shape detection. Computer Graphics Forum, 26(2), 214-226 (2007).
20. Torr, P. H. S., Zisserman, A.: MLESAC: A New Robust Estimator with Application to Estimating Image Geometry. Computer Vision and Image Understanding, 78(1), 138-156 (2000).